Critical-Point Boundary for the Nuclear Quantum Phase Transition Near $A = 100$ from Mass Measurements of ^{96,97}Kr

S. Naimi,[1] G. Audi,[1] D. Beck,[2] K. Blaum,[3] Ch. Böhm,[3] Ch. Borgmann,[3] M. Breitenfeldt,[4,*] S. George,[3,†] F. Herfurth,[2] A. Herlert,[5] M. Kowalska,[3] S. Kreim,[3] D. Lunney,[1,‡] D. Neidherr,[6] M. Rosenbusch,[4] S. Schwarz,[7] L. Schweikhard,[4] and K. Zuber[8]

[1]*CSNSM-IN2P3-CNRS, Université de Paris Sud, 91405 Orsay, France*
[2]*GSI Helmholtzzentrum für Schwerionenforschung GmbH, 64291 Darmstadt, Germany*
[3]*Max-Planck-Institut für Kernphysik, 69117 Heidelberg, Germany*
[4]*Ernst-Moritz-Arndt-Universität, Institut für Physik, 17487 Greifswald, Germany*
[5]*CERN, Physics Department, 1211 Geneva 23, Switzerland*
[6]*Johannes Gutenberg-Universität, Institut für Physik, 55099 Mainz, Germany*
[7]*NSCL, Michigan State University, East Lansing, Michigan 48824-1321, USA*
[8]*Institut für Kern- und Teilchenphysik, Technische Universität, 01069 Dresden, Germany*

(Received 16 March 2010; published 16 July 2010)

Mass measurements of ^{96,97}Kr using the ISOLTRAP Penning-trap spectrometer at CERN-ISOLDE are reported, extending the mass surface beyond $N = 60$ for $Z = 36$. These new results show behavior in sharp contrast to the heavier neighbors where a sudden and intense deformation is present. We interpret this as the establishment of a nuclear quantum phase transition critical-point boundary. The new masses confirm findings from nuclear mean-square charge-radius measurements up to $N = 60$ but are at variance with conclusions from recent gamma-ray spectroscopy.

DOI: 10.1103/PhysRevLett.105.032502 PACS numbers: 21.10.Dr, 64.70.Tg, 74.40.Kb

Dynamical symmetries are an enlightening paradigm for describing the stucture of matter. Iachello and Arima have elegantly described the application of dynamic symmetries in nuclear physics by developing the Interacting Boson Model (IBM) [1]. The IBM allowed the classification of nuclear spectra in terms of U(6) group theory and predicted the occurrence of three dynamical symmetries: U(5), SU(3), and SO(6) [2]. More recent attempts to enlarge these concepts have resulted in the elaboration of critical-point symmetries, notably for nuclear shapes [3,4]. These are particularly interesting since they apply to interactions that are discontinuous and describe phenomena in terms of quantum phase transitions. Whereas classical phase transitions follow changes in temperature and pressure, the quantum phase transitions of nuclear shapes occur when neutrons and protons change their orbit occupation in the nucleus.

The IBM formalism describes the ground-state band of a deformed nucleus and in the pure SU(3) limit, has the same definition as a Boson condensate. With the 2001 Nobel prize [5], Bose-Einstein condensates have now become one of the most studied phenomena in physics. Linking the atomic nucleus with dilute gases of ultracold atoms thus offers interesting possibilities for furthering our understanding of nuclear structure. Indeed, the ideas of phase transitions and condensates have been extended to fermionic matter in the form of an α-particle condensation [6], which has profound implications in nucleosynthesis. Another example is the description of halo nuclides, where the alpha phase transition is favored over pairing in the dilute nuclear halo [7]—a striking parallel to Bose-Einstein condensates in dilute gases.

Nuclear quantum phase transitions are linked to ground-state binding energies within the framework of the IBM [1] (for more detailed discussion in the experimental context, see also [8–10]). The ground-state binding energy reflects the net result of all interactions at work in the nucleus and its minimization is decisive for the occupational sequence of the nuclear orbitals. As such, nuclear deformation is highly visible from deep indentations of the mass surface. These features are the manifestations of a first-order quantum phase transition with the critical points defining where the phase transition starts and where it ends [11].

In this Letter, we report new mass measurements in the $Z = 40$ and $N = 60$ region of the nuclear chart, where one of the most remarkable examples of nuclear shape transition (both for its intensity and its suddenness) is found. Its discovery [12] spawned extensive experimental and theoretical exploration, chronicled in [13–15].

Figure 1 shows the mass surface defined by the isotopic two-neutron separation energies S_{2n} (the binding energy difference between isotopes with N and $N - 2$ neutrons), which illustrates the deformation in the region of interest. Most of the mass data was present in the 2003 Atomic-Mass Evaluation [16] but was extended and considerably refined thanks to Penning-trap measurements by ISOLTRAP [17] and JYFLTRAP [18,19]. The present masses of ^{96,97}Kr establish the limit of the region of strong deformation and allow, for the first time, mapping the lower boundary of the region of critical-point behavior. It also vividly shows how mass measurements can provide

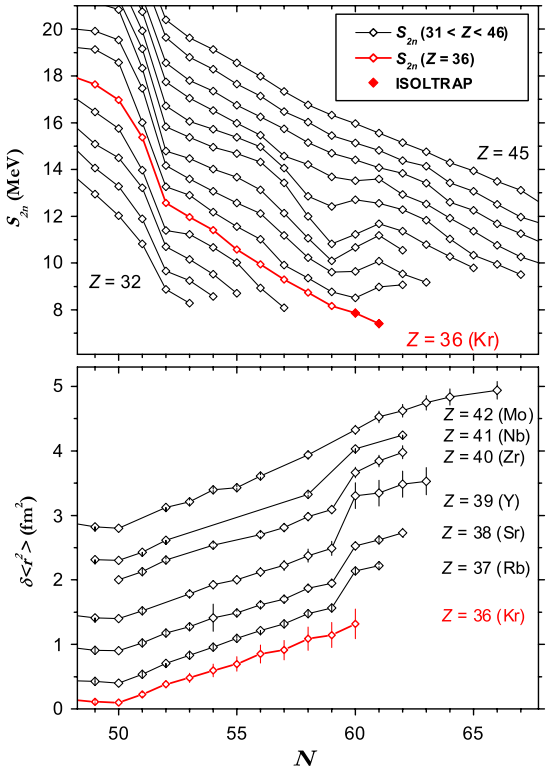

FIG. 1 (color online). (Top panel) Two-neutron separation energies (S_{2n}) for $Z = 32$–45 versus N. The new Kr data reported here are represented by filled diamonds (error bars smaller than the points). Other data from [16], complemented by [17] for Kr; [18] for Sr, Mo, and Zr; and [19] for Y and Nb. (Bottom panel) Difference in mean-square charge radii for the $N = 60$ region. Data are from [28] for Kr, [39] for Rb, [40,41] for Sr, [29] for Y, [30] for Zr, [31] for Nb, and [32] for Mo.

key structural information that is usually garnered only after extensive spectroscopy. Shown in the lower panel of Fig. 1 are mean-square charge radii, obtained by high-resolution laser spectroscopy, for many of the same isotopic chains. The sudden changes seen in the binding energies are also reflected by the radii, as discussed below.

The measurements were performed with the Penning-trap mass spectrometer ISOLTRAP [20] located at the isotope-separator facility ISOLDE at CERN. The Kr nuclides were produced by irradiating a 50 g/cm^2 uranium-carbide target with pulses of 1.4-GeV protons from CERN's Proton Synchrotron Booster accelerator. The nuclear reaction products diffused from the hot target through a water-cooled transfer line into the new versatile arc-discharge ion source [21]. The singly-charged ions were transported at 30 keV through the two-stage high-resolution mass separator into the ISOLTRAP cooler-buncher where they were prepared for capture into the cylindrical Penning trap. Usually, high precision mass measurements are carried out in the second, hyperbolic-shaped precision Penning trap where the cyclotron frequency $\nu_c = qB/(2\pi m)$ (q and m are the charge and the mass of the ion, respectively, and B is the magnetic field of the trapped ion is measured via the established time of flight ion-cyclotron-resonance detection technique [22]. This was indeed the case for ^{96}Kr [see Fig. 2, top panel]. Because of the much lower yield of ^{97}Kr, exacerbated by its particularly short half-life ($T_{1/2} = 63$ ms) and the high charge-exchange rate of Kr ions with the residual gas, only the first (preparation) trap was used to measure the mass of this nuclide. There, a mass-selective ion-centering procedure [23] is applied before extracting and transporting the ions to a detector for counting. The theoretical line shape of the cyclotron-resonance peaks from the preparation trap has not (yet) been fully described. In the past, fits to a Gaussian form have been used (see, e.g., [24–26]). Given the proper conditions, the thermalized ions are centered in the preparation trap. When they are extracted through the 3-mm aperture in the end cap electrode, the expected detected-ion profile as a function of centering frequency should be a step function. However, the ion distribution results in a flat profile with smoothed edges.

The ^{97}Kr spectrum [Fig. 2, bottom panel] was analyzed using a Gaussian fit as well as a symmetric, flattened fit (inspired by the Woods-Saxon nuclear potential) with frequency, offset, amplitude, width, and wall smoothness as free parameters. Additionally, the frequency center and variance of the ion distributions were determined using a

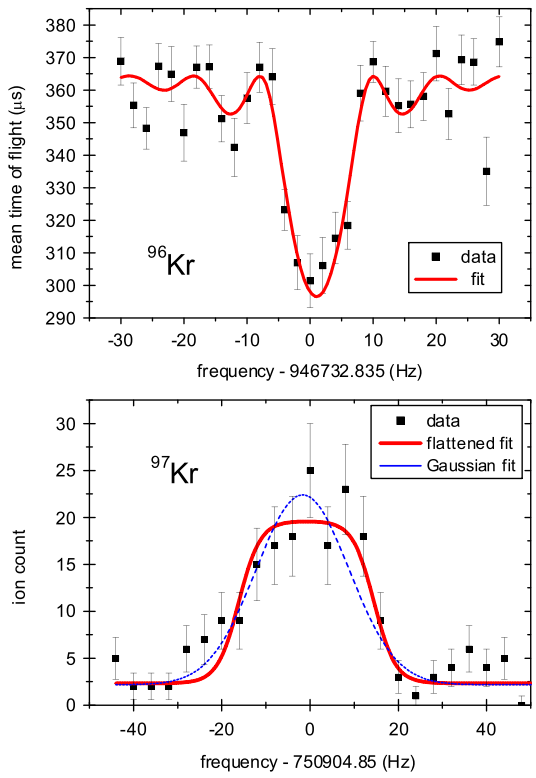

FIG. 2 (color online). (Top panel) Time of flight recorded for ^{96}Kr ejected from the precision trap and (bottom panel) ion counts for ^{97}Kr ejected from the preparation trap, as a function of excitation frequency.

TABLE I. Frequency ratios $r = \nu_{c,\mathrm{ref}}/\nu_c$, mass excesses D of the measured Kr isotopes, and differences Δ where those masses are known. The reference-ion mass excesses are $D(^{85}\mathrm{Rb}) = -82\,167.331(11)$ keV [16] and $D(^{86}\mathrm{Kr}) = -83\,265.6234(56)$ keV [27].

A	$r = \nu_{c,\mathrm{ref}}/\nu_c$	D (keV)	Δ (keV)	Citation
	Precision trap	^{85}Rb reference ion		
80	0.941 168 89(11)	−779 04(9)	11(9)	[16]
87	1.023 572 463(55)	−807 08(4)	−2(4)	[16]
94	1.106 255 84(28)	−613 81(22)	33(22)	[17]
96	1.129 914 80(26)	−530 80(20)		This work
	Preparation trap	^{85}Rb reference ion		
86	1.011 763 9(103)	−832 04(82)	−62(82)	[27]
94	1.106 255 6(114)	−613 96(91)	48(91)	[17]
	Preparation trap	^{86}Kr reference ion		
94	1.093 392 94(125)	−614 75(100)	127(100)	[17]
97	1.128 488 72(159)	−474 28(130)		This work

third, algebraic method (i.e., with no *a priori* assumption on the distribution shape). This latter procedure yielded the smallest uncertainty but is sensitive to the frequency window and to how the background is subtracted. The flattened-distribution fit yields a lower χ^2 than the Gaussian, which is expected since it has more free parameters. Both are robust concerning background and window. The center frequencies derived from the three different methods all agree within their respective uncertainties. In the following, we use the flattened distribution. The detailed description of this procedure will be the subject of a future publication.

While mass measurements using a preparation trap were reported by JYFLTRAP [24] and SHIPTRAP [25], this is the first such measurement for ISOLTRAP. Therefore, additional cross checks were performed using the same nuclide in each trap. In order to calibrate the magnetic fields at the time of the measurement, a reference-mass cyclotron frequency was measured immediately before and after that of the ion of interest. All measured frequency ratios are listed in Table I with derived mass excesses.

The cold transfer line from the target only allows gaseous species to reach the ion source so that the beam arriving at the experiment is of good purity. However, noble gas ions readily charge exchange with impurities present in buffer gas. Therefore, in the case of the preparation-trap measurements, we also used a reference ion having the same chemical properties (^{86}Kr). Added to this problem was the short half-lives, which meant that the ions often beta decayed while in the trap. The emitted beta particles further ionized the residual gas, creating contamination *in situ*. Indeed, the Kr mass measurements in the preparation trap show frequency shifts with ion number, most likely due to the presence of decay and charge-exchange products. Adding an uncertainty of 1×10^{-6} in quadrature with the statistical uncertainty for these cases allowed for a 1σ agreement between cross-check measurements. This uncertainty is included in the corresponding frequency ratios of Table I. The preparation-trap masses for ^{86}Kr and ^{94}Kr agree quite well with those in the literature and the mass measurement of ^{94}Kr made with the precision trap deviates by only 33 (22) keV from the previous ISOLTRAP value [17]. Moreover, the ^{94}Kr mass values measured with both Penning traps also agree. An additional preparation-trap cross-check was performed by measuring ^{133}Cs with respect to ^{85}Rb ($r = 1.565\,221\,22(174)$) resulting in a reassuring agreement of −29(44) keV with respect to the well-known ^{133}Cs mass. The masses for ^{96,97}Kr (Table I) are the first for these nuclides.

The two new S_{2n} values resulting from these measurements are indicated by solid points in Fig. 1. Contrary to the heavier isotopic chains, where an increase in S_{2n} indicates a gain in binding energy due to deformation, the S_{2n} values for Kr continue to decrease steadily with N. The behavior in this new area of the mass surface is in marked contrast with that shown by isotopes with higher Z. A ''normal'' linear trend only starts to be reestablished for the $Z = 42$ (Mo) isotopes. Thus the critical points delimiting the area of the quantum phase transition appear quite clearly.

Additional support for this conclusion comes from comparing the new results with other observables. First, optical isotope-shift measurements by Keim *et al.* [28] [see Fig. 1] revealed that the mean-square charge-radius of ^{96}Kr ($N = 60$) did not significantly increase with respect to ^{95}Kr. This is in stark contrast with the heavier isotopic chains of Sr and Rb. Subsequent laser spectroscopy work on Y [29], Zr [30], and Nb [31] has also corroborated the dramatic shape change at $N = 60$. As in the case of Kr, both masses and recently measured Mo charge radii also smooth out when crossing the border region near $N = 60$, giving credence to the idea of a critical point [32].

γ-ray spectroscopy of microsecond isomers of ^{95}Kr was performed with the Lohengrin spectrometer at ILL by Genevey *et al.* [33] who found that spherical shape predominates (at least at low energy) already at $N = 59$ for Kr. Coulomb excitation of ^{92}Kr performed at REX-ISOLDE [34] revealed an increased $E2$ strength and hence,

enhanced quadrupole collectivity at the $N = 56$ $d_{5/2}$ subshell closure in contrast to previous conclusions [35]. This subshell is clearly visible from the mass surface in Fig. 1 for $Z = 37$–42. The disappearance of this subshell for ^{92}Kr was illustrated by the ISOLTRAP mass measurements of Delahaye *et al.* [17] and corroborates the REX-ISOLDE results. A γ-ray study of ^{96}Kr, recently performed at Legnaro with the PRISMA spectrometer and CLARA clover array by Marginean *et al.* [36], reported an excited state with a very low energy of 241 keV. Their assignment of this state to the first 2^+ state, though advanced with great caution, would be indicative of rather strong deformation and thus, a conclusion at odds with the masses and charge radii.

Accompanying the discovery of this deformation region was the statement that ^{96}Kr would "most likely" have the same deformation as the neighboring nuclides [12]. It is interesting to point out that the first microscopic calculations of shapes in this region [13] predicted the same deformation for ^{96}Kr as for ^{98}Sr and ^{100}Zr. Likewise, recent density-functional-theory calculations using the Gogny force and collective Hamiltonian [37] give a good overall description, but miss the important trends visible in the S_{2n} curves and predict deformation in the Kr isotopes close to that of Zr, with a critical-point boundary at lower Z. Our new binding energies tell a different story.

Apart from the Pb-Ir region, IBM calculations have focused almost exclusively on the collective features present in the $A = 150$ rare-earth region and provide a good picture in terms of a quantum phase transition. The only calculations in the $A = 100$ region were performed for Zr nuclides [38]. As for the heavier region, the IBM calculations of the masses and excited states are nicely described in the framework of a quantum phase transition. It will be very interesting to see if the same calculations can describe the critical-point boundary for the Kr isotopes.

In summary, we have determined the masses of ^{96,97}Kr for the first time. The resulting mass surface reveals the boundaries of critical-point behavior in this pivotal $A \approx 100$ quantum phase transitional region and illustrates anew how powerful Penning-trap mass spectrometry can be in tracing out nuclear structural evolution.

We thank M.-G. Porquet for discussions and R. F. Casten for valuable commentary on the manuscript. We are grateful to the members of the ISOLDE technical group and to the ISOLDE Collaboration for their support as well as the German Federal Ministry for Education (BMBF) through Grants No. 06GF151 and No. 06MZ215; the French IN2P3; the Max-Planck Society; and the Helmholtz Association for National Research Centers (VH-NG-037).

*Present address: IKS-Katholieke Universiteit Leuven, Celestijnenlaan 200D, B-3001 Leuven, Belgium

†Present address: NSCL, Michigan State University, East Lansing, MI 48824-1321, USA

‡Corresponding author: david.lunney@csnsm.in2p3.fr

[1] F. Iachello and A. Arima, *The Interacting Boson Model* (Cambridge University Press, Cambridge, England, 1987).
[2] A. Arima and F. Iachello, Ann. Phys. (Leipzig) **99**, 253 (1976); **111**, 201 (1978); **123**, 468 (1979).
[3] F. Iachello, Phys. Rev. Lett. **85**, 3580 (2000).
[4] F. Iachello, Phys. Rev. Lett. **87**, 052502 (2001).
[5] E. A. Cornell and C. E. Weiman, Rev. Mod. Phys. **74**, 875 (2002); W. Ketterle, Rev. Mod. Phys. **74**, 1131 (2002).
[6] P. Schuck *et al.*, Prog. Part. Nucl. Phys. **59**, 285 (2007).
[7] K. Hagino *et al.*, Phys. Rev. Lett. **99**, 022506 (2007).
[8] J. Jolie, Prog. Part. Nucl. Phys. **59**, 337 (2007).
[9] P. Cejnar and J. Jolie, Prog. Part. Nucl. Phys. **62**, 210 (2009).
[10] R. F. Casten, Prog. Part. Nucl. Phys. **62**, 183 (2009).
[11] O. Scholten, F. Iachello, and A. Arima, Ann. Phys. (Leipzig) **115**, 325 (1978).
[12] S. A. E. Johansson, Nucl. Phys. **64**, 147 (1965).
[13] D. A. Arseniev, A. Sobiczewski, and V. A. Soloviev, Nucl. Phys. **A139**, 269 (1969).
[14] *Nuclear Structure of the Zr Region*, edited by J. Eberth, R. A. Meyer, and K. Sistemich (Springer, Berlin, 1988).
[15] J. Skalski, S. Mizutori, and W. Nazarewicz, Nucl. Phys. **A617**, 282 (1997).
[16] G. Audi, A. H. Wapstra, and C. Thibault, Nucl. Phys. **A729**, 337 (2003).
[17] P. Delahaye *et al.*, Phys. Rev. C **74**, 034331 (2006).
[18] U. Hager *et al.*, Phys. Rev. Lett. **96**, 042504 (2006).
[19] U. Hager *et al.*, Nucl. Phys. **A793**, 20 (2007).
[20] M. Mukherjee *et al.*, Eur. Phys. J. A **35**, 1 (2008).
[21] L. Penescu *et al.*, Nucl. Instrum. Methods Phys. Res., Sect. B **266**, 4415 (2008).
[22] M. König *et al.*, Int. J. Mass Spectrom. Ion Process. **142**, 95 (1995).
[23] G. Savard *et al.*, Phys. Lett. A **158**, 247 (1991).
[24] V. Kolhinen *et al.*, Nucl. Instrum. Methods Phys. Res., Sect. A **528**, 776 (2004).
[25] S. Rahaman *et al.*, Int. J. Mass Spectrom. **251**, 146 (2006).
[26] M. Kowalska *et al.*, Eur. Phys. J. A **42**, 351 (2009).
[27] W. Shi, M. Redshaw, and E. G. Myers, Phys. Rev. A **72**, 022510 (2005).
[28] M. Keim *et al.*, Nucl. Phys. **A586**, 219 (1995).
[29] B. Cheal *et al.*, Phys. Lett. B **645**, 133 (2007).
[30] P. Campbell *et al.*, Phys. Rev. Lett. **89**, 082501 (2002).
[31] B. Cheal *et al.*, Phys. Rev. Lett. **102**, 222501 (2009).
[32] F. C. Charlwood *et al.*, Phys. Lett. B **674**, 23 (2009).
[33] J. Genevey *et al.*, Phys. Rev. C **73**, 037308 (2006).
[34] D. Mücher *et al.* in *13th Capture Gamma-Ray Spectroscopy Conference*, edited by A. Blazhev (American Institute of Physics, Cologne, Germany, 2009), Vol. CP1090, p. 587.
[35] G. Lhersonneau *et al.*, Phys. Rev. C **63**, 034316 (2001).
[36] N. Marginean *et al.*, Phys. Rev. C **80**, 021301(R) (2009).
[37] J.-P. Delaroche *et al.*, Phys. Rev. C **81**, 014303 (2010).
[38] J. E. Garcia-Ramos *et al.*, Eur. Phys. J. A **26**, 221 (2005).
[39] C. Thibault *et al.*, Phys. Rev. C **23**, 2720 (1981).
[40] F. Buchinger *et al.*, Phys. Rev. C **41**, 2883 (1990).
[41] P. Lievens *et al.*, Phys. Lett. B **256**, 141 (1991).